Atmos. Chem. Phys. Discuss., 14, 16387–16409, 2014
www.atmos-chem-phys-discuss.net/14/16387/2014/
doi:10.5194/acpd-14-16387-2014


Atmospheric Chemistry and Physics
Discussions
Open Access



# Stratospheric winds: longitudinal distribution and long-term trends

**M. Kozubek, P. Krizan, and J. Lastovicka**

Institute of Atmospheric Physics ASCR, Bocni II, 14131 Prague, Czech Republic

Received: 19 April 2014 – Accepted: 10 June 2014 – Published: 20 June 2014

Correspondence to: M. Kozubek (kom@ufa.cas.cz)

Published by Copernicus Publications on behalf of the European Geosciences Union.







Stratospheric winds: longitudinal distribution and long-term trends

M. Kozubek et al.

## Abstract

The wind is very important parameter of the stratospheric dynamics which can be affected by many factors like tropospheric North Atlantic Oscillation (NAO) or El Nino Southern Oscillation (ENSO), stratospheric Quasi-biennial Oscillation (QBO) or Sudden Stratospheric Warming (SSW) and solar activity. Due to lack of direct observations we have to use reanalysis data, here NCEP/NCAR reanalysis. The behaviour and trends of wind and its meridional component is analysed in this paper. The influence of NAO on trend in wind is significant in the lower stratosphere (100 hPa) in Atlantic sector; the trend is also affected by QBO, whereas influence of SSW is rather minor and observable only in the middle stratosphere (10 hPa). The most interesting result seems to be the longitudinal distribution of the meridional wind component. We identify two-core structure of strong but opposite winds, one at each hemisphere at 10 hPa, and a four-core structure at 100 hPa. These structures are not associated with tides. However, they appear to be related to the well-pronounced Aleutian pressure high at the 10 hPa level.

## 1 Introduction

The Upper Troposphere/Lower Stratosphere (UTLS) region represents a link for the troposphere-stratosphere coupling as well as for chemistry-climate coupling (e.g. Shepherd, 2007). Stratospheric winds play a main role in stratospheric chemistry through transporting long-lived species, but they also could create transport barriers which could isolate the polar vortex in winter (Shepherd, 2007, 2008). Simultaneously with chemical processes, trace gas distribution moderates the radiative forcing in stratospheric region. The changes of stratospheric wind (strengthening of westerly polar vortex and its poleward shift) are coupled with ozone depletion and temperature changes. The possible interaction between changes in the stratosphere dynamics and climate changes in the troposphere has been described by Hartmann et al. (2000).

That is why it is important to understand the stratospheric circulation and the impact of climate change on this circulation.

The stratospheric Quasi-biennial Oscillation (QBO) and downward feedback from the stratospheric vortex to tropospheric weather systems have also been reported to be relevant both in the context of weather prediction and climate (Baldwin and Dunkerton, 1999; Baldwin et al., 2003; Sigmond et al., 2008; Marshall and Scaife, 2009; Wang and Chen, 2010). Moreover, stratospheric wind affects vertically propagating atmospheric waves which control the transport circulation in the stratosphere and mesosphere (Holton and Alexander, 2000). That is why we are going to study the behaviour, trend and connection of winds to the other phenomena of middle latitude stratosphere and show their impact on climate and troposphere behaviour.

The stratospheric winds in meteorological analyses and reanalyses have some problems when we compare them with observations (e.g., Kozubek et al., 2014). One of the reasons is that winds in reanalyses are derived from primarily calculated quantities (i.e. geopotential height distribution). We usually replace unobserved variables, which the stratospheric wind is, by observed ones through the use of balance relationships. For example the application of a mass-wind balance (Derber and Bouttier, 1999) leads to a state in which the large number of temperature soundings provides a strong constraint on the balanced wind component, i.e. approximately the geostrophic wind (Baron et al., 2013). However, it is hard to derive the larger scale wind fields using the geostrophic assumption especially in the tropical region because the Coriolis parameter vanishes at the equator and the solutions become numerically unstable (Hamilton, 1998; Žagar et al., 2004; Polavarapu et al., 2005).

Despite the importance of middle atmospheric observations, wind measurements, which are assimilated in the models, are mostly limited to the troposphere. In the mesosphere, winds are measured using optical techniques from satellites (Shepherd et al., 1993; Hays et al., 1993; Killeen et al., 1999; Niciejewski et al., 2006), by ground-based radar systems such as European Incoherent SCATter (EISCAT) (Alcayde and Fonta-





ACPD
14, 16387–16409, 2014

nari, 1986) and various meteor and other radars (Maekawa et al., 1993; Jacobi et al., 2009).

Baron et al. (2013) suggest that winds can be derived down to 40 km by using emission lines from other molecules but they show that reliable measurement using this method can be done only for higher levels (higher than 50 km). Other studies confirm these results. That is why Baron et al. (2013) recommend this method for observations above the 50 km. Stratospheric winds have been measured from the ground using active and passive techniques (Hildebrand et al., 2012; Rufenacht et al., 2012) and from space by the High Resolution Doppler Imager (HRDI) on UARS covering 10–35 km and 60° S–60° N, using the molecular oxygen A- and B-bands (Ortland et al., 1996).

In this paper we analyze the connection of stratospheric wind to the other phenomena like Quasi-biennial Oscillation (QBO), Sudden Stratospheric Warming (SSW) or North Atlantic Oscillation (NAO). Next we look at the distribution of meridional wind component in the different pressure levels and try to find the possible reason for its behaviour.

The structure of the paper is as follows. In Sect. 2 the data and methods are described. Then, in Sect. 3 the results of analysis are shown and in Sect. 4 briefly discussed. Section 5 provides the conclusions.

## 2 Data and methods

We have used NCEP/NCAR-1 reanalysis (further on NCEP/NCAR). The NCEP/NCAR reanalysis was described in detail by Kistler et al. (2001). This reanalysis provides data from 1948 onwards, but data is more reliable from 1957 onwards, when the first upper-air observations were established, and from 1979 onwards, due to the beginning of satellite date assimilation. Data is available in the 2.5° to 2.5° grid at 00:00, 06:00, 12:00 and 18:00 UTC. Vertical resolution is 28 levels with the top of the model at 2.7 hPa. The NCEP/NCAR analysis system efficiently assimilates upper-air observations but it is only marginally influenced by surface observations be-





ACPD
14, 16387–16409, 2014

Stratospheric winds: longitudinal distribution and long-term trends

M. Kozubek et al.

cause model orography differs from reality (Kistler et al., 2001). According to Kozubek et al. (2014) winds from the NCEP/NCAR reanalysis reveal the best results when compare with ERA-40 and ERA-Interim reanalysis or observations at Prague-Libus, ERA-40 has a problem with wind speed and direction distributions at 10 hPa in the last four years (1998–2002) and ERA-Interim agreement with observations is slightly worse than that of NCEP/NCEP reanalysis. Moreover, neither ERA-40, nor ERA-Interim separately covers the whole period 1970–2012. That is why we can consider NCEP/NCAR reanalysis reliable and adequate for our analyses. The 10.7 cm radio solar flux (from http://www.esrl.noaa.gov/psd/data/correlation/solar.data) is used for the solar cycle analysis (solar max and solar min). The QBO data at 50 hPa is taken from http://www.geo.fu-berlin.de/en/met/ag/strat/produkte/qbo/.

The analysis has been done for wind speed data from 30° N to 80° N but in this paper we are mainly focused on middle latitudes (50°, 52.5°, 55° N) at two pressure levels 100 and 10 hPa. These two pressure levels represent the dynamics and conditions in the lower (100 hPa) and middle (10 hPa) stratosphere at middle latitudes. The three selected latitudes represent middle latitude band from 49° N to 56° N. We analyzed them separately to show the detail changes in each of the three latitudes but usually the results are quite similar, therefore we present them predominantly only for one latitude. We mostly use daily data from 00:00 UTC but for one analysis we have to choose also 06:00 and 12:00 UTC (analysis of diurnal and semidiurnal tides). The selected latitudes are separated into four sectors (0–90° E – European sector, 90–180° E – Asian sector, 180–300° W – Pacific-American sector, and 300–360° E – Atlantic sector). The wind speed is calculated from gridded u and v components. In analyses we have used either total wind, or u (zonal) and v (meridional) components separately.

We look for time development in each sector at both pressure levels. The statistical significance threshold of trends has been set on 95 % level (using standard MATLAB routine). We compare behaviour of wind speed in different sectors. Then we divide data of the whole period into several groups according to QBO, NAO or solar cycle influence. We again compute trends separately for all these groups with significance threshold 95 %. These analyses have been done for total wind speed or for u and v components, respectively.

We have computed averages through the whole period (1970–2012) for every grid point from 20° N to 60° N and for every month. Comparison of wind speed distribution in 100 and 10 hPa at 00:00 UTC or wind speed distribution at 00:00, 06:00 and 12:00 UTC (06:00 and 12:00 for analysis of diurnal and semidiurnal tides) separately for u and v components has been done.

## 3 Results

### 3.1 Long-term trends in winds

In this section we would like to show the influence of different stratospheric/ tropospheric phenomena on the stratospheric wind speed. Figure 1 shows time development of winter averages (October–March) of wind speed for different sectors of 52.5° N. We have done analysis also for other latitudes (50° N and 55° N) and the results were very similar (not shown here). On the top panel we can see results for 100 hPa. The behaviour of Atlantic sector (300–360° W) is different from other sectors (Pacific, European). There is significant positive trend (95 % level) from 1970 till 1996 and negative trend after 1996 in the Atlantic sector. The peak value of wind speed and turnaround of trend in 1996 coincide with the total ozone trend turnaround in northern middle latitudes (e.g., Harris et al., 2008). The trends in other three sectors are also insignificant. Generally stronger winds occur in Atlantic sector, especially after 1985. At pressure level 10 hPa no significant trend can be found. The behaviour is rather chaotic and qualitatively similar for all four sectors. There are stronger winds in Atlantic (300–360° W) and European (0–360° E) sectors, in some years the wind is two times stronger in Atlantic than Asian sector (42 $m\,s^{-1}$ and 17 $m\,s^{-1}$, respectively for 1998).

Due to different behaviour in Atlantic sector we compare time series of wind speed and NAO index. NAO is selected because it influences the winds in Atlantic sector in





ACPD
14, 16387–16409, 2014

troposphere and its effect could be observed even in the lower stratosphere. Figure 2 shows the results. The trends in winds and NAO for three different periods (1958–1970, 1971–1995 and 1996–2009) are similar in tendency, an insignificant negative trend before 1970, a significant positive trend for 1970–1995, and a significant negative trend after 1995. Thus winds at 100 hPa in Atlantic sectors are influenced by NAO much more than in other sectors, which do not display a significant trend. This is physically plausible results.

Now we show winter (December–February only) trends for two periods (1970–1995 and 1995–2012). This analysis will show us the influence of different stratospheric phenomena (QBO or SSW) on the stratospheric winds (dynamics). We have to start at 1970 because before this year the reliability of NCEP/NCAR reanalysis data is lower (Kozubek et al., 2014). We use daily data and that is why these two periods (25 and 17 years) should be long enough for our analyses. The results are presented in Table 1. We divide data into several groups. The first two groups show results for winters when either major SSW occurs or does not occur. This analysis should reveal the influence of major SSW on dynamics in different sectors of middle latitudes. Some statistically significant trends (95 % level) at 100 hPa for all three analysed latitudes are found mainly in the Atlantic sector. Generally positive trend is seen in 1970–1995 and negative one in 1995–2012 which agree with previous studies. At 10 hPa there are no statistically significant trends for group with major SSWs but again a positive tendency in 1970–1995 and a negative tendency in the second period are observed. The second group without major SSWs reveals again positive tendency in the first period and negative one in the second. However, we can find several significant trends in both periods, even though weaker than corresponding trends at 100 hPa. These results indicate that major SSWs at 10 hPa support a tendency to absence of significant trends (change of wind during the major SSW). No substantial impact of major SSWs on trends in winds is found for 100 hPa; trends with and without major SSWs are very similar.

The third and fourth groups in Table 1 show trends for years when the east or west phase of QBO occur, respectively. At 100 hPa we can found significant trend mainly





ACPD
14, 16387–16409, 2014

for period 1970–1995 in Atlantic and European sectors. Again we can found change from positive (in the first period) to negative (in the second period) trends, which is well pronounced for the west phase of QBO, whereas there is no systematic change for the east phase of QBO. There is no typical behaviour at 10 hPa for the east or west phase of QBO. At 10 hPa the tendency to change from positive (1970–1995) to negative (1995–2012) trends can be seen for both phases of QBO but again it is more pronounced for the west phase of QBO. There are almost no differences between trends in the east and west QBO phases for positive trends in 1970–1995 but negative trends in 1995–2010 in European and Atlantic sectors are much more negative for the west phase of QBO. Thus the results show that for both pressure levels trends and their change in the mid-1990s are evidently better pronounced for the west than east phase of QBO. We have done similar analysis separately for each month; the results are similar to the whole winter results (December–February).

### 3.2 Impact of solar cycle on winds

Another analysis, which has been done, is comparison between years in the solar cycle maximum and minimum in different QBO phases. This analysis will show the connection between solar cycle and stratospheric dynamics (QBO and wind speed). Stratospheric dynamics and chemistry is influenced by solar activity especially at higher levels. Again we show winter (October–March) averages but we have also results from each winter month. The results for absolute wind speed are shown on the first two panels of Table 2. At 10 hPa we can observe a difference between solar maximum and minimum for the west QBO. The wind speed in solar minimum is stronger (by 2–5 $\mathrm{m\,s^{-1}}$) than in solar maximum especially in European and Atlantic sectors. The east QBO does not reveal a systematic difference; moreover sometimes wind in solar maximum is stronger than in solar minimum. At 100 hPa if there are some differences, they are mainly for the east QBO, not west like at 10 hPa. The two bottom panels show the same analysis as top ones but for v (meridional) wind component. An analysis for zonal wind component may be found in many studies but we have not found in literature such an analysis for meridional component. At 10 hPa we observe slightly stronger winds in solar minimum than solar maximum for the east QBO. At 100 hPa we cannot find any significant differences for both phases of QBO. This analysis was done also for each month and the biggest differences of absolute wind speed and v component were found in December and January. These results confirm that solar activity influence mainly higher part of the stratosphere.

### 3.3 Longitudinal distribution of stratospheric meridional winds

Because we have found different signs in different sectors during the previous analysis of meridional wind component (see Table 2, bottom panels), we have computed the whole possible period (1958–2012) averages of this component for each grid point from 60° N to 20° N for January and/or July, respectively. The results are shown in Figs. 3 and 4. The top panel show results for 10 hPa and bottom for 100 hPa. Figure 3 reveals at 10 hPa a strong poleward wind on the east hemisphere of the middle and higher latitudes. This poleward wind changes into equatorward on the west hemisphere at 10 hPa (similar amplitude as on the east hemisphere). Generally winds are stronger at 10 hPa (up to 20 $\mathrm{m\,s^{-1}}$) than at 100 hPa (up to 10 $\mathrm{m\,s^{-1}}$). At 100 hPa there are two cores with negative (equatorward) and two cores with positive (poleward) values. The same analysis, but for July, is shown on Fig. 4. This analysis shows that the observed feature occurs only in winter. The winds are weaker than in January and the distribution is much less compact compared with January, especially at 10 hPa, whereas at 100 hPa there is again a tendency to four core patterns but at lower latitudes than in January. We have done the same analysis for higher pressure levels (up to 5 hPa) and the differences between east and west hemisphere have been growing with increasing height.

Figure 5 show averages through period 1957 to 2012 for January at 10 hPa pressure level but we compare data from 00:00 UTC (top panel), 06:00 UTC (middle panel) and 12:00 UTC (bottom panel). There are almost no differences in main features. That is why we can conclude that the two core structure with opposite meridional winds is not





ACPD
14, 16387–16409, 2014

caused by diurnal or semidiurnal tides. The other possibility for this structure could be dynamical reasons which are discussed in the next paragraph.

Figure 6 shows a distribution of geopotential height at 10 and 100 hPa. The Aleutian pressure high centred at about 40–55° N, 180° E is well developed at 10 hPa. This height can block the zonal winter eastward winds. This results in poleward winds on front side and in equatorward winds on the backside as a consequence of flow along this massive anticyclone. This coincides with the observed two core structure at 10 hPa with the poleward meridional component of wind on the eastern hemisphere and the equatorward meridional component on the western hemisphere. At 100 hPa at least on the western hemisphere (not at eastern one) the distribution of geopotential height (Fig. 6) seems to support the four core structure in winds (Fig. 3). The summertime distribution of geopotential heights at 10 hPa does not display any well-pronounced structure and, therefore, no pronounced structure is developed in meridional wind (Fig. 4).

## 4 Discussion

Our results, which concern higher middle latitudes, coincide with the result of Scaife et al. (2005) that NAO as a tropospheric phenomenon affects zonal winds in the lower stratosphere (and vice versa); we added to that finding that contrary to the lower stratosphere, trends in winds in the middle stratosphere (10 hPa) are not influenced significantly by NAO. Our results also show that QBO as a stratospheric phenomenon, which influences the stratosphere at all heights, affects trends at both the 100 and 10 hPa levels, whereas major sudden stratospheric warming (SSW), which is substantially better developed at 10 hPa than at 100 hPa, affect trends measurably only at 10 hPa. The influence of QBO and SSWs and their combination on the stratosphere has been discussed in many papers, e.g. recently by Watson and Gray (2014). The influence of QBO on global stratospheric circulation, so called Holton-Tan effect, has first been observed by Holton and Tan (1980).





ACPD
14, 16387–16409, 2014

Perhaps the most interesting result offers the analysis of geographic distribution of meridional component of stratospheric wind in the form of the well-pronounced two-core structure at 10 hPa in winter. The meridional wind has not been studied often. We have not found in literature any analysis of its geographic distribution without zonal mean averaging. The wintertime longitudinal distribution at 10 hPa can be explained neither by diurnal, nor by semidiurnal tides, because there are no differences between the longitudinal distribution of meridional winds at 00:00, 06:00 and 12:00 UTC (Fig. 5). However, the geopotential height analysis reveals a possible reason for this longitudinal distribution. The well-developed large Aleutian high at 10 hPa in Fig. 6 can block the zonal flow and pushes winter eastward winds to flow poleward on western side of the Aleutian pressure high and back equatorward on its eastern side. This is in qualitative agreement with the behaviour of meridional wind in Fig. 3. This feature can at least partly explain the longitudinal distribution of winds at 10 hPa. As for 100 hPa, the distribution of geopotential heights at the western hemisphere seems to support the observed four-core longitudinal distribution of winds but such effect is largely absent at the eastern hemisphere. Further investigations of origin of the two- and four-core longitudinal structure of stratospheric winds will be done in near future but even these basic results show that we have to be careful when zonal mean averages are used for analyses, because in such a way we can miss important information.

## 5 Conclusions

Analysis of wintertime midlatitude NCEP/NCAR reanalysis data at 100 and 10 hPa levels in higher middle latitudes reveals noticeable influence of stratospheric (QBO) and tropospheric (NAO) phenomena on the trends in winds in the stratosphere. It also exhibits a reversal of trends in winds in the mid-1990s in accord with change of trend in ozone. A remarkably stronger trends in wind observed at 100 hPa (not at 10 hPa) in Atlantic sector are related to trends in NAO. Even though NAO is a tropospheric phenomenon, it can affect the dynamics at least in the lower stratosphere. The effect of

QBO, which means much more pronounced trend and its change in the west phase of QBO than in the east phase, is evident in both pressure levels. Major sudden stratospheric warmings (SSWs) support tendency to absence of significant trends in winds at 10 hPa; they have no substantial impact on trends in winds at 100 hPa.

Another analysis is comparison of stratospheric winds in the winter northern middle latitudes between years of the solar cycle minimum and maximum under different QBO conditions. The results differ for 100 and 10 hPa and for total or meridional wind (Table 2), so a clear overall pattern cannot be established.

The analysis of geographic distribution of meridional component of stratospheric wind in winter is shown in Fig. 3 for 20–60° N. It reveals well pronounced longitudinal distribution of winds at latitudes above 30–35° N with two cores of strong but opposite meridional winds, one at each hemisphere (eastern and western) at 10 hPa, and a somewhat less pronounced four-core structure at 100 hPa. In summer such a well-pronounced core structure is absent (Fig. 4). The two-core structure at 10 hPa is not caused by tides as it is demonstrated by Fig. 5. We have identified the strong and well-developed large Aleutian pressure high at 10 hPa Fig. 6, which appears to contribute to the two-core structure and which is capable to explain qualitatively this structure.

*Acknowledgements.* Authors acknowledge support by the Grant Agency of the Czech Republic, grant P209/10/1792, by the Ministry of Education, Youth and Sports of the Czech Republic, grant LD 12070, and by the COST ES1005 project (TOSCA).

## References

Alcayde, D. and Fontanari, J.: Neutral temperature and winds from EISCAT cp-3 observations, J. Atmos. Terr. Phys., 48, 931–947, 1986.

Baron, P., Murtagh, D. P., Urban, J., Sagawa, H., Ochiai, S., Kasai, Y., Kikuchi, K., Khosrawi, F., Körnich, H., Mizobuchi, S., Sagi, K., and Yasui, M.: Observation of horizontal winds in the middle-atmosphere between 30° S and 55° N during the northern winter 2009–2010, Atmos. Chem. Phys., 13, 6049–6064, doi:10.5194/acp-13-6049-2013, 2013.





ACPD

14, 16387–16409, 2014

Baldwin, M. P. and Dunkerton, T. J.: Propagation of the arctic oscillation from the stratosphere to the troposphere, J. Geophys. Res., 104, 30937–30946, 1999.
Baldwin, M., Shuckburgh, D. Norton, E., Thompson, W., and Gillett, G.: Weather from the stratosphere?, Science, 301, 317–318, 2003.
Derber, J. and Bouttlier, F.: A reformulation of the background error covariance in the ECMWF global data assimilation system, Tellus A, 51, 195–221, 1999.
Hamilton, K.: Dynamics of the tropical middle atmosphere: a tutorial review, Atmos. Ocean, 36, 319–354, 1998.
Harris, N. R. P., Kyrö, E., Staehelin, J., Brunner, D., Andersen, S.-B., Godin-Beekmann, S., Dhomse, S., Hadjinicolaou, P., Hansen, G., Isaksen, I., Jrrar, A., Karpetchko, A., Kivi, R., Knudsen, B., Krizan, P., Lastovicka, J., Maeder, J., Orsolini, Y., Pyle, J. A., Rex, M., Vanicek, K., Weber, M., Wohltmann, I., Zanis, P., and Zerefos, C.: Ozone trends at northern mid- and high latitudes – a European perspective, Ann. Geophys., 26, 1207–1220, doi:10.5194/angeo-26-1207-2008, 2008.
Hartmann, D. L., Wallace, J. M., Limpasuvan, V., Thompson, D. W., and Holton, J. R.: Can ozone depletion and global warming interact to produce rapid climate change?, P. Natl. Acad. Sci. USA, 97, 1412–1417, 2000.
Hays, P. B., Dobbs, V. J., Gell, M. E., Grassl, D. A., Abreu, H. J., and Skinner, W. R.: The high-resolution Doppler imager on the upper-atmosphere research satellite, J. Geophys. Res., 98, 10713–10723, 1993.
Hildebrand, J., Baumgarten, G., Fiedler, J., Hoppe, U.-P., Kaifler, B., Lübken, F.-J., and Williams, B. P.: Combined wind measurements by two different lidar instruments in the Arctic middle atmosphere, Atmos. Meas. Tech., 5, 2433–2445, doi:10.5194/amt-5-2433-2012, 2012.
Holton, J. R. and Alexander, M. J.: The role of waves in transport circulation of the middle atmosphere, Geoph. Monog. Series, 123, 21–35, 2000.
Holton, J. R. and Tan, H.-C.: The influence of the equatorial quasi-biennial oscillation on the global circulation at 50 mb, J. Atmos. Sci., 37, 2200–2208, 1980.
Jacobi, C., Kurschner, C., Singer, D., Homann, W., Arras, P., and Keuer, D.: Comparison of mesopause region meteor radar winds, medium frequency radar winds and low frequency drifts over Germany, Adv. Space Res., 43, 247–252, 2009.
Killeen, T. L., Johnson, W. R., Edmonson, R. M., Wu, C. J., Niciejewski, Q., Grassl, R. J., Gell, H. J., Hansen, D. A., Harvey, P. E., Skinner, J. D., and Kafkalidis, J. F.: Timed Doppler

Interferometer (TIDI), optical spectroscopic techniques and instrumentation for atmospheric and space research, Proc. SPIE, 3756, 289–301, 1999.
Kistler, R., Collins W. Kalnay, E., Saha, S., White, G., Woollen, J., Muthuvel, C., Ebisuzaki, W., Kanamitsu, M., Kousky, V., van den Dool, H., Jenne, R., and Fiorino, M.: The NCEP 50-year reanalysis: monthly means CDrom and documentation, B. Am. Meteorol. Soc., 82, 247–267, 2001.
Kozubek, M., Laštovička, J., and Križan, P.: Differences in mid-latitude stratospheric winds between reanalysis data and versus radiosonde observations at Prague, Ann. Geophys., 32, 353–366, doi:10.5194/angeo-32-353-2014, 2014.
Maekawa, Y., Yamamoto, S., Yamanaka, M., Tsuda, M. D., Kato, T., Fukao, S., and Woodman, R. F.: First observation of the upper stratospheric vertical wind velocities using the Jicamarca HF radar, J. Geophys. Res., 111, A11S90, doi:10.1029/93GL02606, 1993.
Marshall, A. G. and Scaife, A. A.: Impact of QBO on surface winter climate, J. Geophys. Res., 114, D18110, doi:10.1029/2009JD011737, 2009.
Niciejewski, R., Skinner, Q., Gell, W., Cooper, D., Marshall, M., Killeen, A., Solomon, T., Wu, S., and Ortland, D.: Timed Doppler interferometer on the thermosphere ionosphere mesosphere energetics and dynamics satellite: data product overview, J. Geophys. Res., 111, A11S90, doi:10.1029/2005JA011513, 2006.
Ortland, D. A., Skinner, W. R., Hays, P. B., Burrage, M. D., Lieberman, R. S., Marshall, A. R., and Gell, D. A.: Measurements of stratospheric winds by the High Resolution Doppler Imager, J. Geophys. Res., 101, 10351–10363, 1996.
Polavarapu, S., Rochon, T. G., Shepherd, Y., and Ren, S.: Some challenges of middle atmosphere data assimilation, Q. J. Roy. Meteor. Soc., 131, 3513–3527, 2005.
Rüfenacht, R., Kämpfer, N., and Murk, A.: First middle-atmospheric zonal wind profile measurements with a new ground-based microwave Doppler-spectro-radiometer, Atmos. Meas. Tech., 5, 2647–2659, doi:10.5194/amt-5-2647-2012, 2012.
Scaife, A. A., Knight, J. R., Vallis, G. K., and Folland, C. K.: A stratospheric influence on the winter NAO and North Atlantic surface climate, Geophys. Res. Lett., 32, L18715, doi:10.1029/2005GL023226, 2005.
Shepherd, G. G., Gault, G., Solheim, W. A., Hersom, B. H., Alunni, C., Brun, J. M., Brune, J. F., Charlot, S., Cogger, P., Desaulniers, L. L., Evans, D. L., Gattinger, W. F. J., Girod, R. L., Harvie, F., Hum, D., Kendall, R. H., Llewellyn, D. J. W., Lowe, E. J., Ohrt, R. P., Pasternak, J., Peillet, F., Powell, O., Rochon, I., Ward, Y., Wiens, W. E., Thuillier, R. H., and Wimperis, J.:

Windii, the wind imaging interferometer on the upper-atmosphere research satellite, J. Geophys. Res., 98, 10725–10750, 1993.
Shepherd, T. G.: Transport in the middle atmosphere, J. Meteorol. Soc. Jpn. II, 85B, 165–191, 2007.
Shepherd, T. G.: Dynamics, stratospheric ozone, and climate change, Atmos. Ocean, 46, 117–138, 2008.
Sigmond, M., Scinocca, J. F., and Kushner, P. J.: Impact of the stratosphere on the tropospheric climate change, Science, 301, 317–318, 2008.
Wang, L. and Chen, W.: Downward arctic oscillation signal associated with moderate weak stratospheric polar vortex and the cold December 2009, Geophys. Res. Lett., 37, L09707, doi:10.1029/2010GL042659, 2010.
Watson, P. A. G. and Gray, L. J.: How does the quasi-biennial oscillation affect the stratospheric polar vortex?, J. Atmos. Sci., 71, 391–409, 2014.
Zagar, N., Gustafsson, N., and Kallen, E.: Variational data assimilation in the tropics: the impact of a background-error constraint, Q. J. Roy. Meteor. Soc., 130, 103–125, 2004.





ACPD
14, 16387–16409, 2014

Stratospheric winds: longitudinal distribution and long-term trends

M. Kozubek et al.

**Table 1.** Winter (December–February only) trends ($m\,s^{-1}$ per year) of total wind speed for two periods (1970–1995 and 1996–2012). Major SSW – only years when the major SSW (according to WMO definition) occur, no SSW – years when no SSW occurs, east QBO – only years when the east phase of QBO occurs, west QBO – only years when the west phase of QBO occurs. Top panel 100 hPa, bottom panel 10 hPa. 70–95 means 1970–1995 and 95–12 means 1995–2012. Significant trends on 95 % level are highlighted by bold numbers.

| 100 hPa | | | | | | | | | | | | | |
|---|---|---|---|---|---|---|---|---|---|---|---|---|---|
| latitude | 50° N | | | | 52.5° N | | | | 55° N | | | | |
| sector | 0–90 | 90–180 | 180–300 | 300–360 | 0–90 | 90–180 | 180–300 | 300–360 | 0–90 | 90–180 | 180–300 | 300–360 | |
| 70–95 | **0.07** | −0.02 | 0.06 | **0.15** | 0.06 | −0.04 | 0.06 | **0.16** | 0.05 | −0.02 | 0.06 | **0.12** | major SSW |
| 95–12 | −0.13 | 0.00 | −0.22 | **−0.60** | −0.15 | 0.01 | −0.26 | **−0.64** | −0.18 | −0.05 | −0.29 | **−0.57** | major SSW |
| 70–95 | 0.11 | 0.04 | 0.09 | 0.20 | 0.12 | −0.01 | **0.14** | 0.27 | 0.11 | −0.01 | 0.09 | 0.25 | no SSW |
| 95–12 | −0.14 | −0.01 | −0.19 | **−0.55** | −0.09 | −0.06 | **−0.18** | **−0.53** | −0.12 | 0.00 | −0.26 | **−0.55** | no SSW |
| 70–95 | **0.10** | **−0.18** | −0.01 | 0.09 | 0.07 | **−0.20** | −0.02 | **0.09** | 0.06 | **−0.18** | −0.03 | 0.09 | east QBO |
| 95–12 | −0.26 | **0.10** | 0.08 | **−0.35** | −0.26 | **0.07** | 0.04 | −0.43 | −0.27 | 0.00 | −0.01 | **−0.48** | east QBO |
| 70–95 | **0.05** | 0.02 | **0.11** | **0.26** | 0.08 | 0.03 | **0.14** | **0.28** | 0.10 | 0.04 | 0.15 | **0.28** | west QBO |
| 95–12 | 0.04 | 0.05 | −0.27 | **−0.54** | −0.06 | −0.08 | **−0.36** | **−0.62** | −0.18 | −0.22 | −0.43 | **−0.68** | west QBO |

| 10 hPa | | | | | | | | | | | | | |
|---|---|---|---|---|---|---|---|---|---|---|---|---|---|
| | 50° N | | | | 52.5° N | | | | 55° N | | | | |
| | 0–90 | 90–180 | 180–300 | 300–360 | 0–90 | 90–180 | 180–300 | 300–360 | 0–90 | 90–180 | 180–300 | 300–360 | |
| 70–95 | 0.00 | 0.05 | 0.03 | 0.01 | −0.01 | 0.07 | 0.04 | 0.04 | −0.01 | 0.09 | 0.05 | 0.08 | major SSW |
| 95–12 | 0.16 | −0.06 | −0.25 | −0.16 | 0.08 | −0.11 | −0.28 | −0.21 | −0.02 | −0.13 | −0.31 | −0.26 | major SSW |
| 70–95 | 0.05 | 0.04 | 0.09 | **0.11** | 0.00 | 0.07 | 0.08 | **0.14** | 0.07 | **0.14** | 0.04 | **0.17** | no SSW |
| 95–12 | −0.07 | **−0.15** | **−0.19** | −0.06 | −0.08 | 0.00 | **−0.24** | −0.12 | 0.06 | −0.07 | **−0.20** | **−0.18** | no SSW |
| 70–95 | **0.16** | 0.15 | 0.02 | 0.11 | **0.22** | 0.17 | 0.04 | 0.20 | **0.29** | 0.20 | **0.08** | 0.29 | east QBO |
| 95–12 | 0.15 | −0.27 | −0.33 | 0.07 | 0.00 | −0.31 | **−0.40** | −0.07 | −0.19 | −0.31 | −0.47 | −0.26 | east QBO |
| 70–95 | **0.23** | 0.04 | 0.10 | **0.22** | **0.22** | 0.05 | 0.11 | **0.26** | 0.20 | 0.07 | 0.12 | **0.28** | west QBO |
| 95–12 | −0.43 | −0.36 | −0.21 | −0.55 | **−0.56** | −0.45 | −0.25 | **−0.60** | **−0.65** | −0.51 | −0.32 | **−0.65** | west QBO |





ACPD
14, 16387–16409, 2014

**Table 2.** Winter (October–March) averages of wind speed ($m s^{-1}$) for different latitudes and sectors. Top panels total wind speed for two pressure level, bottom panel v (meridional) wind component for two pressure levels. Min-east: years under solar minimum and the east phase of QBO conditions; min-west: years under solar minimum and the west phase of QBO, the same for solar maximum conditions.

| | 50° N | | | | 52.5° N | | | | 55° N | | | | latitude |
|---|---|---|---|---|---|---|---|---|---|---|---|---|---|
| | 0–90 | 90–180 | 180–300 | 300–360 | 0–90 | 90–180 | 180–300 | 300–360 | 0–90 | 90–180 | 180–300 | 300–360 | sector |
| min-east | 33.24 | 21.13 | 19.38 | 28.40 | 34.68 | 23.02 | 20.44 | 29.66 | 35.76 | 25.11 | 21.85 | 30.76 | 10 hPa |
| max-east | 32.62 | 20.09 | 20.74 | 29.55 | 34.70 | 22.12 | 21.63 | 31.15 | 36.47 | 24.43 | 22.79 | 32.56 | |
| min-west | 34.31 | 21.16 | 20.83 | 31.03 | 36.61 | 23.34 | 22.27 | 33.18 | 38.54 | 25.84 | 24.01 | 35.09 | |
| max-west | 32.29 | 20.65 | 19.28 | 28.20 | 34.05 | 22.54 | 20.47 | 29.43 | 35.39 | 24.70 | 21.99 | 30.68 | |
| min-east | 18.30 | 20.94 | 18.81 | 19.99 | 18.60 | 19.12 | 18.39 | 20.39 | 18.98 | 17.88 | 18.11 | 20.67 | 100 hPa |
| max-east | 16.91 | 20.03 | 17.61 | 18.51 | 17.21 | 18.10 | 16.94 | 18.70 | 17.64 | 16.85 | 16.46 | 18.74 | |
| min-west | 18.28 | 21.05 | 18.35 | 18.95 | 18.48 | 19.23 | 17.83 | 19.25 | 18.76 | 17.94 | 17.43 | 19.48 | |
| max-west | 18.23 | 20.92 | 17.57 | 18.42 | 18.56 | 19.04 | 16.95 | 18.52 | 18.92 | 17.70 | 16.50 | 18.56 | |
| min-east | 1.59 | 7.23 | −6.02 | −2.00 | 1.29 | 8.74 | −6.78 | −2.25 | 0.84 | 10.23 | −7.60 | −2.56 | 10 hPa v |
| max-east | 1.39 | 6.84 | −5.80 | −1.23 | 1.20 | 8.25 | −6.61 | −1.41 | 0.85 | 9.66 | −7.49 | −1.64 | |
| min-west | 1.60 | 7.87 | −6.62 | −1.71 | 1.40 | 9.47 | −7.57 | −1.95 | 1.10 | 11.06 | −8.62 | −2.25 | |
| max-west | 1.77 | 6.69 | −5.89 | −1.66 | 1.60 | 8.11 | −6.71 | −2.00 | 1.28 | 9.50 | −7.63 | −2.33 | |
| min-east | −2.82 | 1.46 | 0.14 | 2.34 | −3.35 | 1.83 | −0.04 | 2.78 | −3.86 | 2.34 | −0.25 | 3.16 | 100 hPa v |
| max-east | −2.94 | 1.53 | −0.04 | 2.73 | −3.43 | 1.91 | −0.25 | 3.19 | −3.91 | 2.47 | −0.50 | 3.56 | |
| min-west | −2.84 | 1.49 | −0.11 | 2.86 | −3.38 | 1.93 | −0.41 | 3.47 | −3.91 | 2.51 | −0.75 | 4.00 | |
| max-west | −2.80 | 1.40 | 0.20 | 2.29 | −3.28 | 1.75 | 0.05 | 2.67 | −3.75 | 2.27 | −0.17 | 2.98 | |





ACPD
14, 16387–16409, 2014

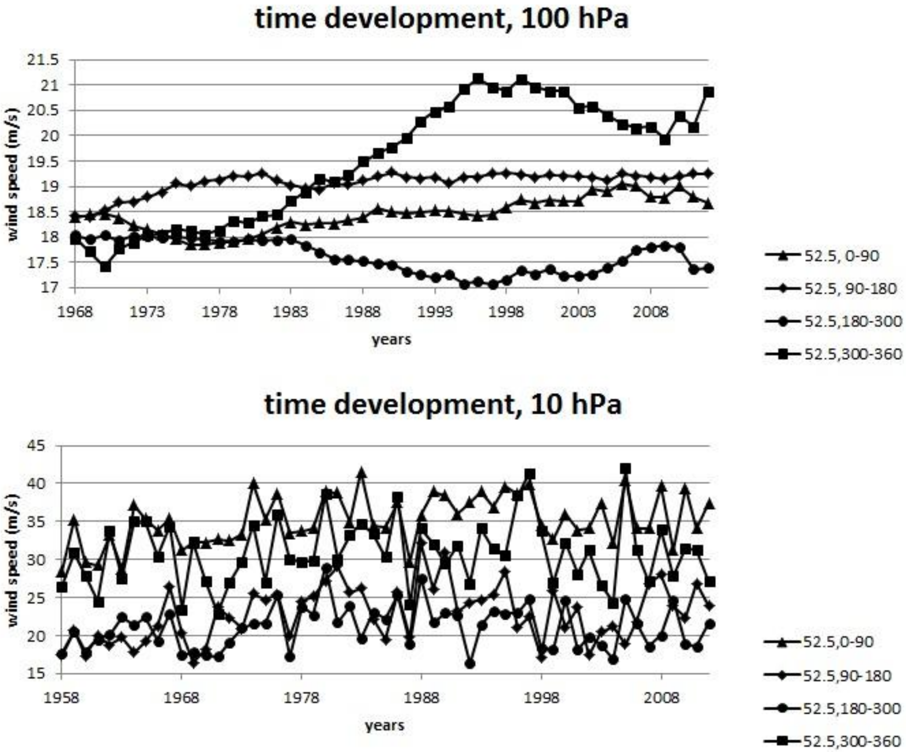


**Figure 1.** Time development – winter averages (October–March) of wind speed in four different sectors of 52.5° N for period 1958–2012. Top panel is for 100 hPa, bottom panel for 10 hPa.





ACPD
14, 16387–16409, 2014

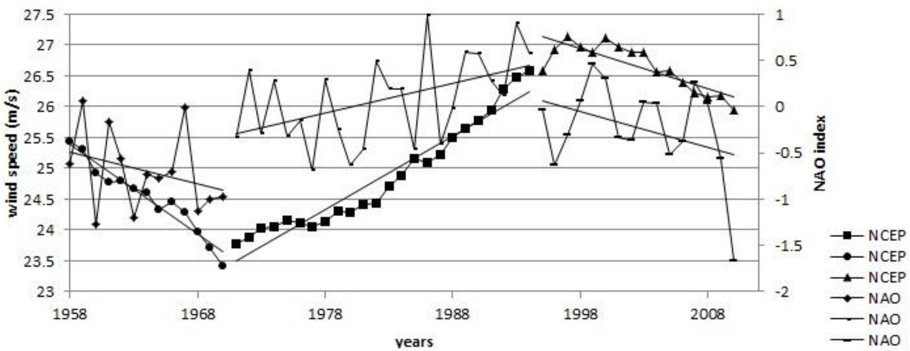


**Figure 2.** Comparison of wind speed at 100 hPa, 52.5° N, sector 300–360° E and NAO index for three different periods.

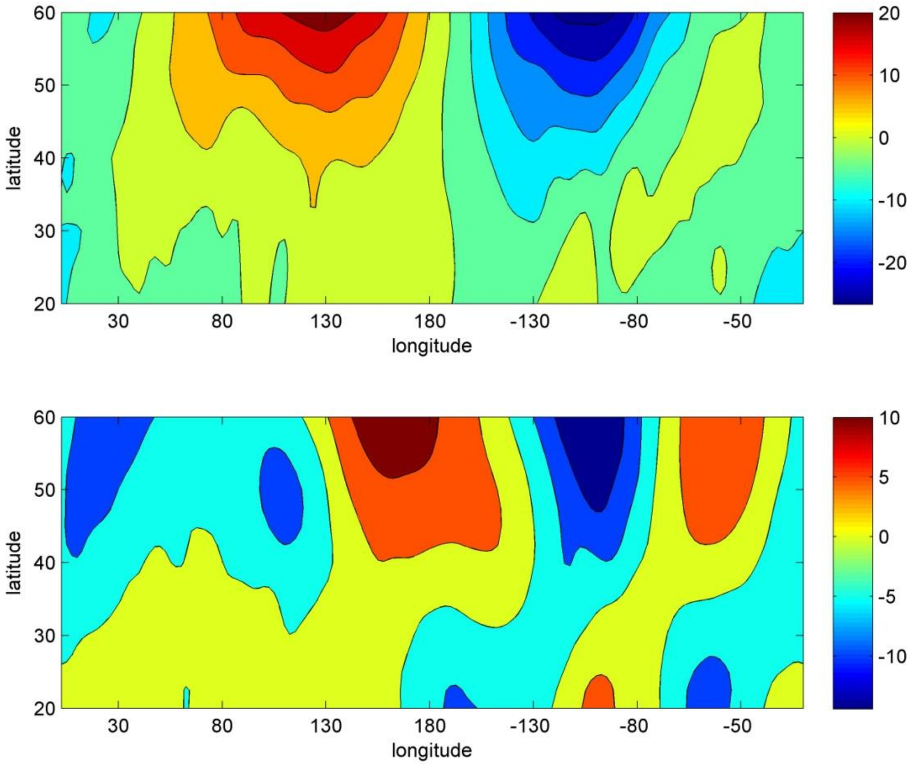


**Figure 3.** Plot of average meridional wind speed ($m\,s^{-1}$) component for January, 1958–2012, 20–60° N, 180° E–180° W. Top panel 10 hPa, bottom 100 hPa.



ACPD
14, 16387–16409, 2014

Stratospheric winds: longitudinal distribution and long-term trends

M. Kozubek et al.

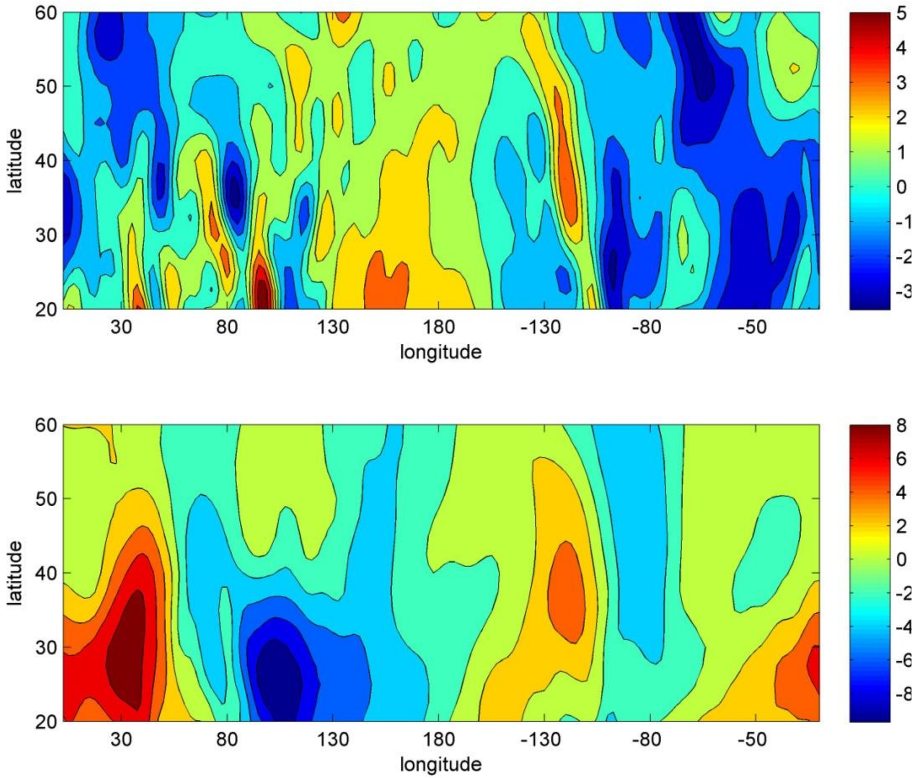


**Figure 4.** The same as Fig. 3 but for July.



ACPD
14, 16387–16409, 2014

Stratospheric winds: longitudinal distribution and long-term trends

M. Kozubek et al.

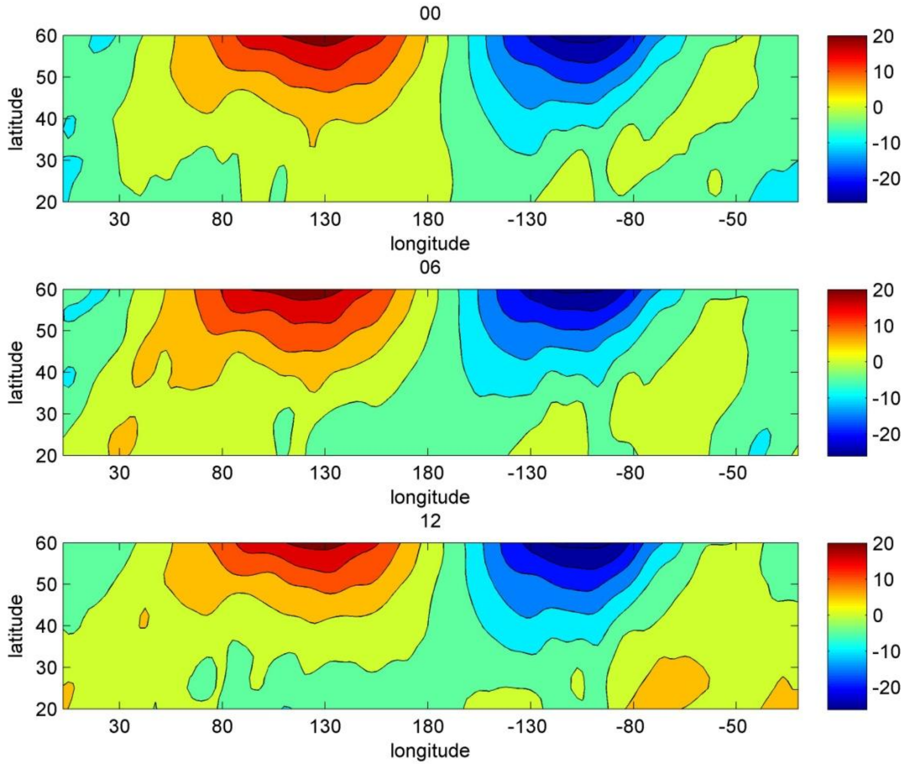


**Figure 5.** Plot of average meridional wind speed ($m\,s^{-1}$) component at 10 hPa for January, 1958–2012, 20–60° N, 180° E–180° W. Top panel 00:00 UTC, middle 06:00 UTC, bottom 12:00 UTC.

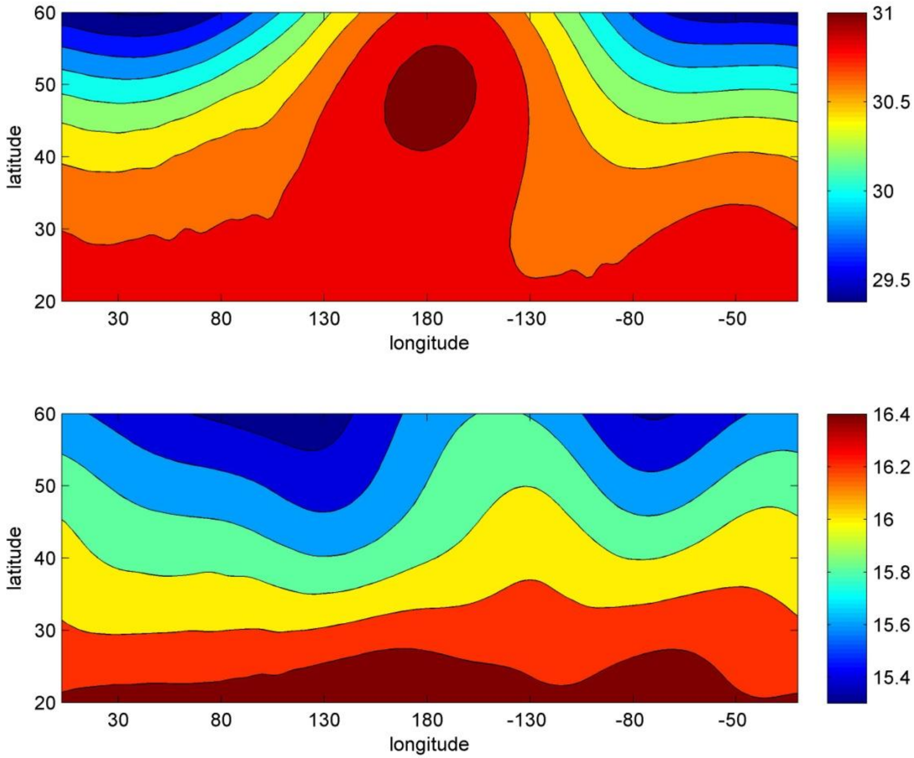


**Figure 6.** Plot of average geopotential height (km) for January, 1958–2012, 20–60° N, 180° E–180° W. Top panel 10 hPa, bottom 100 hPa.





ACPD
14, 16387–16409, 2014